

# **(NH<sub>4</sub>)<sub>3</sub>HfF<sub>7</sub>: crystalloptical and calorimetric studies of a number of successive phase transitions.**

Evgeniy Pogoreltsev<sup>\*ab</sup>, Evgeniy Bogdanov<sup>ac</sup>, Svetlana Melnikova<sup>a</sup>, Igor Flerov<sup>ab</sup>, Nataly Laptash<sup>d</sup>

<sup>a</sup> Kirensky Institute of Physics, Federal Research Center KSC SB RAS, 660036 Krasnoyarsk, Russia

<sup>b</sup> Institute of Engineering Physics and Radioelectronics, Siberian Federal University, 660041 Krasnoyarsk, Russia

<sup>c</sup> Institute of Engineering Systems and Energy, Krasnoyarsk State Agrarian University, 660049 Krasnoyarsk, Russia

<sup>d</sup> Institute of Chemistry, Far Eastern Department of RAS, 690022 Vladivostok, Russia

Single crystals of (NH<sub>4</sub>)<sub>3</sub>HfF<sub>7</sub> were grown. Polarising optical observations as well as measurement of the heat capacity and birefringence  $\Delta n(T)$  were performed in the temperature range of 200–310 K. Reversible phase transitions at temperatures  $T_0 = 290$  K,  $T_1 = 280.5$  K,  $T_2 \approx 273$  K,  $T_3 = 266$  K,  $T_4 = 259$  K,  $T_5 = 231$  K,  $T_6 = 229$  K were found. Observations in polarised light make it possible to suggest a sequence of changes in the symmetry groups for these transitions:  $Fm\bar{3}m \leftarrow T_0 \rightarrow \text{cub.} \leftarrow T_1 \rightarrow \text{mmm (1)} \leftarrow T_2 \rightarrow \text{mmm (2)} \leftarrow T_3 \rightarrow \text{mmm (3)} \leftarrow T_5 \rightarrow 2/c$ . The T-p phase diagram was studied and the temperature boundaries of the stability of the distorted crystalline phases were determined. A significant change of the entropy at successive phase transitions  $\Sigma\Delta S = 10.6$  J/mol·K indicates a disordering of the initial cubic phase.

## **1 Introduction**

A large family of crystals with the elpasolite structure combines substances with structural complexes of different coordination. The compounds with octahedral anionic polyhedra MX<sub>6</sub> (M = Al, Fe, Ti, Zr, Nb, Mo, W; X = O, F, Cl) are well studied [1]. Crystals with a seven-coordinated anion MX<sub>7</sub><sup>3-</sup>, which have a symmetry of  $Fm\bar{3}m, Z = 4$ , are also very interesting. There are several variants of the structure of these substances. The authors of [2]

consider that the oxofluor complex of the crystal  $(\text{NH}_4)_3\text{Ti}(\text{O}_2)\text{F}_5$  is an octahedron, of which one of the apexes is occupied by two oxygen atoms, forming a dumbbell O-O. In favour of this option there are experiments [3] that have shown that as the symmetry decreases as a result of two phase transitions, the fourth-order axis of the crystal remains. The model of the oxofluor complex  $(\text{NH}_4)_3\text{Ti}(\text{O}_2)\text{F}_5$  proposed in [2] was confirmed by recent structural studies [4]. At the same time, there is the opinion that the structure of this substance is constructed from complexes in the form of a pentagonal bipyramid [5].

Among the crystals with the general formula  $\text{A}_3\text{MeX}_7$ , there is a class of substances in which the seventh halogen does not belong to the anionic polyhedron, but occupies a special position in the structure. In the crystal lattice of this compound, a combination of the anions  $\text{MeX}_6^{2-}$  and  $\text{X}^-$  is observed and their chemical formula is represented as corresponding to double salt  $\text{A}_2\text{MeX}_6 \cdot \text{AX}$ . Some of these substances have tetragonal symmetry at room temperature: for example  $\text{K}_3\text{SiF}_7$  [6],  $(\text{NH}_4)_3\text{SiF}_7$  [7],  $(\text{NH}_4)_3\text{GeF}_7$  [8]; while the other have cubic symmetry:  $(\text{NH}_4)_3\text{SnF}_7$  [9],  $(\text{NH}_4)_3\text{PbF}_7$  [10]. In a number of these crystals, phase transitions with an unusual sequence of symmetry changes have been observed [11].

A structural complex in the form of a pentagonal bipyramid is realized in the isostructural fluorine compounds  $(\text{NH}_4)_3\text{HfF}_7$  and  $(\text{NH}_4)_3\text{ZrF}_7$  [4,12]. The crystals have the structure of an ordered perovskite (elpasolite) at ambient conditions with a cubic face-centred lattice (the space group, sp. gr.  $Fm\bar{3}m$ ) in which the F ions form a pentagonal bipyramid around Zr(Hf), having 24 equivalent orientations. References [13,14] contain information about the implementation of a complex sequence of five non-ferroelectric phase transitions including a transition between two cubic phases  $Fm\bar{3}m \leftrightarrow F23$  upon the process of cooling the crystal  $(\text{NH}_4)_3\text{ZrF}_7$ .

This paper presents the results of a study on the number of physical properties of the crystal  $(\text{NH}_4)_3\text{HfF}_7$ , whose structure  $Fm\bar{3}m$  was established recently at room temperature [4]. Complex experiments were performed to determine the influence of the chemical pressure

change caused by the replacement of the central atom Hf  $\rightarrow$  Zr on the resistance to temperature and pressure changes of the initial cubic and distorted phases observed in  $(\text{NH}_4)_3\text{ZrF}_7$  [14].

## 2 Experimental section

According to the procedure described in [4], large transparent single crystals of  $(\text{NH}_4)_3\text{HfF}_7$  were grown with an octahedral habit in accordance with cubic symmetry [4] and optically isotropic at room temperature. X-ray diffraction studies showed the absence of impurities and extraneous phases in crystals.

The temperature dependences of birefringence, extinction position and twinning. were investigated using an Axioskop-40 polarisation microscope and a Linkam LTS 350 temperature chamber at the range of 200–310 K. The birefringence  $\Delta n(T)$  of the cut  $(100)_c$  was measured with the Berke compensator method ('Leica') with an accuracy of  $\pm 0.00001$ .

Calorimetric measurements were performed on a differential scanning calorimeter NETZSCH 204 F1 (DSC).

To study the heat capacity, a polycrystalline sample weighing  $\sim 50$  mg was placed in an aluminium container ( $V = 25 \text{ mm}^3$ ). To refine the results, two series of measurements were carried out including calibration of the heat flux in the required temperature range. Calorimetric studies were performed in the temperature range 220–310 K in a helium atmosphere (flow rate 20 ml/min) with a scan rate of  $5 = \text{K/min}$ . To obtain information on the temperature dependence of the heat capacity, the obtained data were compared with the data of the  $C_p(T)$  of sapphire standard.

DSC studies upon heating have shown seven reproducible and significantly different anomalies of the heat capacity  $C_p$  associated with the successive phase transitions were found:  $G_0 (T_0 = 290 \text{ K}) \leftrightarrow G_1 (T_1 = 280 \text{ K}) \leftrightarrow G_2 (T_2 = 272 \text{ K}) \leftrightarrow G_3 (T_3 = 264 \text{ K}) \leftrightarrow G_4 (T_4 = 259 \text{ K}) \leftrightarrow G_5 (T_5 = 233 \text{ K}) \leftrightarrow G_6 (T_6 = 229 \text{ K}) \leftrightarrow G_7$  (Fig. 1). The temperature dependence of  $C_p(T)$  at regions far from the phase transformations was approximated by a polynomial function for determining the lattice  $C_{\text{lat}}$  and the anomalous  $\Delta C_p = C_p - C_{\text{lat}}$  associated with the phase

transitions contributions. The proximity of the heat capacity anomalies on  $C_p(T)$  makes it impossible to determine the individual integral characteristics such as enthalpy  $\Delta H_i = \int \Delta C_p dT$  and entropy  $\Delta S_i = \int (\Delta C_p / T) dT$  changes for all phase transitions. The energy parameters are reliably established only for sets of anomalies related to two groups in the temperature ranges, as follows: a) 200–250 K ( $\Sigma \Delta S_1 = 0.9 \pm 0.12$  J/mol·K;  $\Sigma \Delta H_1 = 220 \pm 30$  J/mol; and b) 250–320 K ( $\Sigma \Delta S_2 = 9.7 \pm 1.3$  J/mol·K;  $\Sigma \Delta H_2 = 2670 \pm 370$  J/mol).

The temperature-pressure phase diagram was studied by differential thermal analysis (DTA) using a highly sensitive Cu-Ge thermocouple, which has a significant thermoelectric power factor of  $\sim 100$   $\mu\text{V/K}$ . A copper container containing a polycrystalline sample with a mass of 0.02–0.03 g and a quartz standard were attached to the opposite junctions of the DTA element. The pressure was created in a high-pressure chamber of the cylinder-piston type with a multiplier. Silicone oil was the medium to transmit the pressure. To measure the pressure and temperature of the sample, a manganine resistance sensor and a copper-constantan thermocouple were used. The error in measuring the temperature and pressure was  $\pm 0.3$  K and  $\pm 10^{-3}$  GPa, respectively. The experiments were carried out in the modes of increasing and decreasing the pressure, which made it possible to study the reproducibility of the obtained results.

The results of studying the effect of external hydrostatic pressure on the phase transitions in compound  $(\text{NH}_4)_3\text{HfF}_7$  are presented in the T-p phase diagram (Fig. 2). At atmospheric pressure, as in the experiments with DSC, there are seven DTA signal anomalies separating the eight temperature regions shown in Fig. 2. The susceptibility of the phase boundaries to the pressure is represented in the form of the corresponding baric coefficients  $dT_i/dp$  in Table 1. Like  $(\text{NH}_4)_3\text{ZrF}_7$  [14], with a slight increase in the hydrostatic pressure, the heat capacity anomaly associated with the transformation  $G_0 \rightarrow G_1$  (at  $T_0$ ) is not fixed, presumably due to its considerable blurring.

The susceptibility of the phase transitions to hydrostatic pressure was relatively low except for  $G_6 \leftrightarrow G_7$ . Due to the difference in the values of the baric coefficients  $dT_{G_5 \leftrightarrow G_6}/dp$  and

$dT_{G_6 \leftrightarrow G_7}/dp$  in the investigated pressure range 0–0.25 GPa (Table 1), the phase  $G_6$  being wedged out at the triple point with the parameters  $p_{trp1} \approx 0.07$  GPa,  $T_{trp1} \approx 237$  K. At  $p > p_{trp1}$  the baric coefficient  $dT_{G_5 \leftrightarrow G_7}/dp$  remained positive and rather large. Linear extrapolation of the phase boundaries  $G_1 \leftrightarrow G_2$  and  $G_2 \leftrightarrow G_3$ , and also  $G_4 \leftrightarrow G_5$  and  $G_5 \leftrightarrow G_7$  suggests that there are two more triple points on the T-p diagram of  $(\text{NH}_4)_3\text{HfF}_7$  with the parameters:  $p_{trp2} \approx 0.33$  GPa,  $T_{trp2} \approx 282$  K and  $p_{trp3} \approx 0.43$  GPa,  $T_{trp3} \approx 252$  K. Despite the difficulties with the fixation of the second-order transition temperature  $G_0 \rightarrow G_1$  under the pressure mentioned above, it is possible to determine the sign of the corresponding pressure coefficient using the data on the heat capacity and preliminary information about the thermal expansion. From the Ehrenfest equation, it follows that  $dT_{G_0 \leftrightarrow G_1}/dp$  is characterized by the positive value in accordance with the signs of the heat capacity anomalies  $\Delta C_p$ , and the coefficient of volumetric thermal expansion  $\Delta\beta > 0$  at  $T_0$ . Summarising the data above about the temperature behaviour of phase transitions under pressure, it can be assumed that a direct transition between the initial  $G_0$  and the low-temperature  $G_7$  phases in  $(\text{NH}_4)_3\text{HfF}_7$  is highly unlikely, as it was also found for  $(\text{NH}_4)_3\text{ZrF}_7$  [14]. The presence of three triple points on the T-p diagram of  $(\text{NH}_4)_3\text{HfF}_7$  in a relatively narrow pressure range of 0–0.5 GPa indicates less resistance of the distorted phases to external pressure compared to  $(\text{NH}_4)_3\text{ZrF}_7$ , where only one triple point was found [14].

Investigations in polarised light were performed on cuts  $(100)_c$  and  $(111)_c$ . It was found that the crystal in  $G_0$  and  $G_1$  phases belongs to cubic symmetry (Fig. 3a, 4a). Upon cooling, an optical anisotropy appears in the plate  $(100)_c$  at  $T_{1\downarrow} = 279$  K (phase  $G_2$ ) and the crystal is divided into banded twins with boundaries along  $[110]$  from the initial cubic phase. A first-order phase transition occurs, accompanied by a change in the crystal syngony. The extinction of various regions of the sample differs: along  $[110]_c$  (Fig. 3b), or in  $[100]_c$  (Fig. 3c). In  $G_3$  phase, the picture of twins does not change (Fig. 3d), but the regions where extinction occurs in  $[100]_c$  expand (Fig. 3e). Below  $T_3$  ( $G_4$  and  $G_5$  phases) optical anisotropy is increased, the interference colour of the twins appears (Fig. 3f) and the sample is completely extinct along  $[100]_c$  (Fig. 3e–

3g). In  $G_6$  and  $G_7$  phases the twinning pattern becomes more complicated, there is no simultaneous complete extinction of the sample and the crystal is cracked. In the nearby regions a small reversal of the optical indicatrix is observed at an angle of  $\pm\varphi \approx 1^\circ$  relative to the direction  $[100]_c$  (Fig. 3h–3i).

Investigations of cut  $(111)_c$  in polarised light show that the third-order axis in the crystal is lost at  $T_{1\downarrow}$  transition. Below this temperature a characteristic structure appeared with three types of twin boundaries which are located at 120 degrees to each other (Fig. 4a–4b).

The results of measuring the temperature dependence of the birefringence are shown in Fig. 5. There are four temperatures at which there are anomalies of  $\Delta n(T)$  separating five phases of the  $(\text{NH}_4)_3\text{HfF}_7$  crystal:  $T_{1\downarrow} = 279$  K,  $T_{1\uparrow} = 280.5$  K;  $T_{2\downarrow} \approx 266$  K,  $T_{2\uparrow} \approx 273$  K;  $T_{3\downarrow} = 252$  K,  $T_{3\uparrow} = 266$  K;  $T_{5\downarrow} = 223$  K,  $T_{5\uparrow} = 231$  K. The phase  $G_1$  of this substance is optically isotropic ( $\Delta n = 0$ ) and in the  $G_2$  phase, there is a very weak anisotropy. In the process of further cooling, birefringence increases gradually far from phase transitions and abruptly at phase transition point. In the region of a distinct anomaly of the heat capacity at  $T_{4\uparrow} = 259$  K, the features of the birefringence behaviour and the change in the twinning pattern are not observed. All four anomalies of  $\Delta n(T)$  have a temperature hysteresis that differs in magnitude, indicating that they belong to first-order transitions.

### 3 Analysis and discussion

The  $C_p(T)$  dependence for  $(\text{NH}_4)_3\text{HfF}_7$  (Fig. 1) shows great similarity with the behaviour of the heat capacity in  $(\text{NH}_4)_3\text{ZrF}_7$  crystal measured by the adiabatic calorimeter method [14], which also showed seven peaks of the heat capacity near the same temperatures. The authors of [14], analysing the data of complex studies, established that only five of seven anomalies were associated with phase transitions with a sequence of symmetry changes: cubic ( $Fm-3m$ ;  $G_0$ ;  $T_0$ )  $\leftrightarrow$  cubic ( $F23$ ;  $G_1$ ;  $T_1$ )  $\leftrightarrow$  orthorhombic ( $Immm$ ;  $G_2$ ;  $T_2$ )  $\leftrightarrow$  monoclinic 1 ( $I2/m$ ;  $G_3$ ;  $T_3$ )  $\leftrightarrow$  triclinic ( $P-1$ ;  $G_4$ ;  $T_4$ )  $\leftrightarrow$  monoclinic 2 ( $G_5$ ). The phase transition at  $T_0$  between two cubic phases, was characterized as the second order transformation with a dome-shaped anomaly of heat

capacity and it was also not detected by optical studies. The total value of the enthalpy change associated with the sequence of transformations in  $(\text{NH}_4)_3\text{ZrF}_7$  is  $\Sigma\Delta H_i = 3900\pm 400$  J/mol [14], and thus it was 35% more than that obtained in this work for  $(\text{NH}_4)_3\text{HfF}_7$  ( $\Sigma\Delta H_i = 2900\pm 400$  J/mol).

Like the  $(\text{NH}_4)_3\text{ZrF}_7$  the number of heat capacity anomalies in the  $(\text{NH}_4)_3\text{HfF}_7$  crystal (Fig. 1) is much more than detected in the optical experiments (Fig. 5). The high-temperature anomaly  $C_p(T)$  at  $T_0 = 290$  K is similar to that observed in  $(\text{NH}_4)_3\text{ZrF}_7$  [14], and also, no optical isotropy disturbances were observed at this temperature point. Therefore, we assume the presence of a phase transition at  $T_0$  between two cubic phases in a crystal  $(\text{NH}_4)_3\text{HfF}_7$ . Further cooling causes a disturbance of the optical isotropy at  $T_1$  and the gradual lowering of symmetry. The twin patterns in phases  $G_2$  and  $G_3$  differ little (Fig. 3b–3e), and are similar to those observed in the orthorhombic *Immm* phase of the crystal  $(\text{NH}_4)_3\text{ZrF}_7$  [14]: the  $[100]_{\text{orth}}$  and  $[010]_{\text{orth}}$  axes of unit cells are located along  $[110]_c$ . The phase transition  $G_2 \rightarrow G_3$  at  $T_2$  is accompanied by the anomalies of  $C_p(T)$  and  $\Delta n(T)$  but does not appear in the observed twinning pattern.

The phases  $G_4$  and  $G_5$  also have an orthorhombic symmetry, but the axes of their unit cells  $[100]_{\text{orth}}$  and  $[010]_{\text{orth}}$  are parallel to  $[100]_c$ , as evidenced by the extinction character. A small reversal of the optical indicatrix relative to the  $[100]_c$  direction is observed in the monoclinic phases  $G_6$  and  $G_7$ .

The results above show a violation of cubic optical isotropy in the crystal  $(\text{NH}_4)_3\text{HfF}_7$ , and the existence of a sequence of symmetry changes below the room temperature as: cubic ( $G_0$ )  $\leftarrow T_0 \rightarrow$  cubic ( $G_1$ )  $\leftarrow T_1 \rightarrow$  orthorhombic 1 ( $G_2$ )  $\leftarrow T_2 \rightarrow$  orthorhombic 2 ( $G_3$ )  $\leftarrow T_3 \rightarrow$  orthorhombic 3 ( $G_4, G_5$ )  $\leftarrow T_4 \rightarrow$  monoclinic ( $G_6, G_7$ ). In a series of phase transformations, only two ferroelastic transitions accompanied by a change in the syngony are found: at  $T_1$  and  $T_5$ . The nature of heat capacity anomalies at  $T_4 = 259$  K and  $T_6 = 229$  K is not established. The symmetry of the phases  $G_3, G_4$  and  $G_5$  is much higher than those in  $(\text{NH}_4)_3\text{ZrF}_7$  [14]. Perhaps this is the reason for the difference in the values of total entropy change in hafnate and zirconate.

## 4 Conclusions

We have studied heat capacity, crystal optical properties and susceptibility to hydrostatic pressure of  $(\text{NH}_4)_3\text{HfF}_7$ . At ambient and high pressure, thermal properties investigated using DSC and DTA under pressure revealed seven anomalies associated most likely with the successive phase transitions similar to those that we found recently in  $(\text{NH}_4)_3\text{ZrF}_7$  [14]. Birefringence and optical twinning studies were able to detect only four phase transitions with the following change of the point groups:  $Fm\bar{3}m \leftarrow T_0 \rightarrow \text{cub.} \leftarrow T_1 \rightarrow mmm$  (1)  $\leftarrow T_2 \rightarrow mmm$  (2)  $\leftarrow T_3 \rightarrow mmm$  (3)  $\leftarrow T_5 \rightarrow 2/c$ . Similar differences between the thermal and optical data were also observed for  $(\text{NH}_4)_3\text{ZrF}_7$ . A change in the chemical pressure associated with the  $\text{Hf} \rightarrow \text{Zr}$  substitution was accompanied by the following:

- 1) an insignificant change in the phase transitions temperatures;
- 2) different symmetry succession of the distorted phases observed in optic studies;
- 3) a decrease in the total entropy change;
- 4) a lower resistance of distorted phases to external pressure.

## Acknowledgements

The reported study was funded by RFBR and Government of Krasnoyarsk Territory according to the research project No. 16-42-243001.

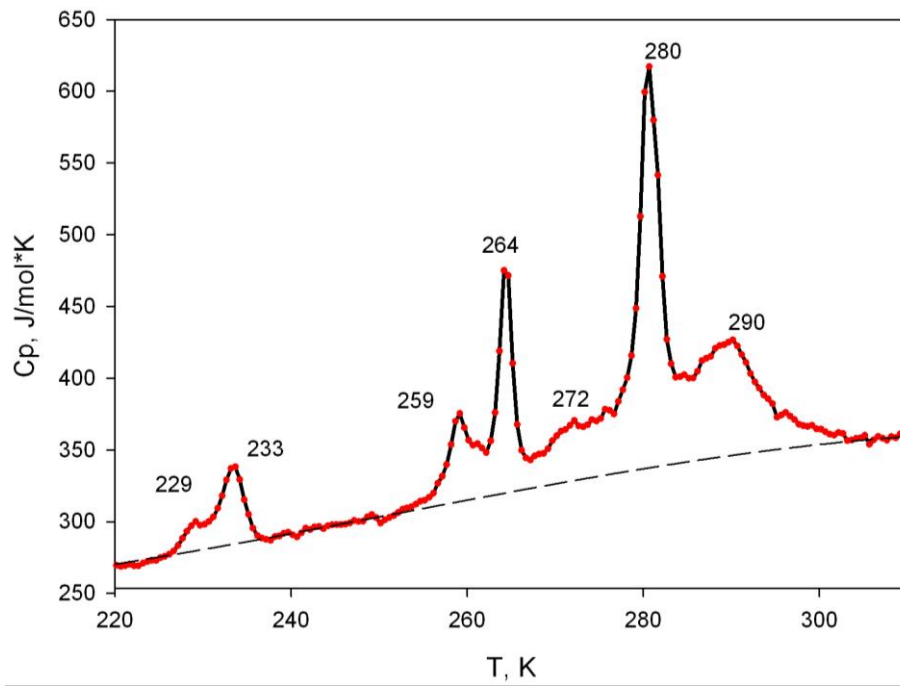


Fig. 1 The temperature dependence of  $C_p(T)$  upon heating. The dashed line shows the lattice heat capacity.

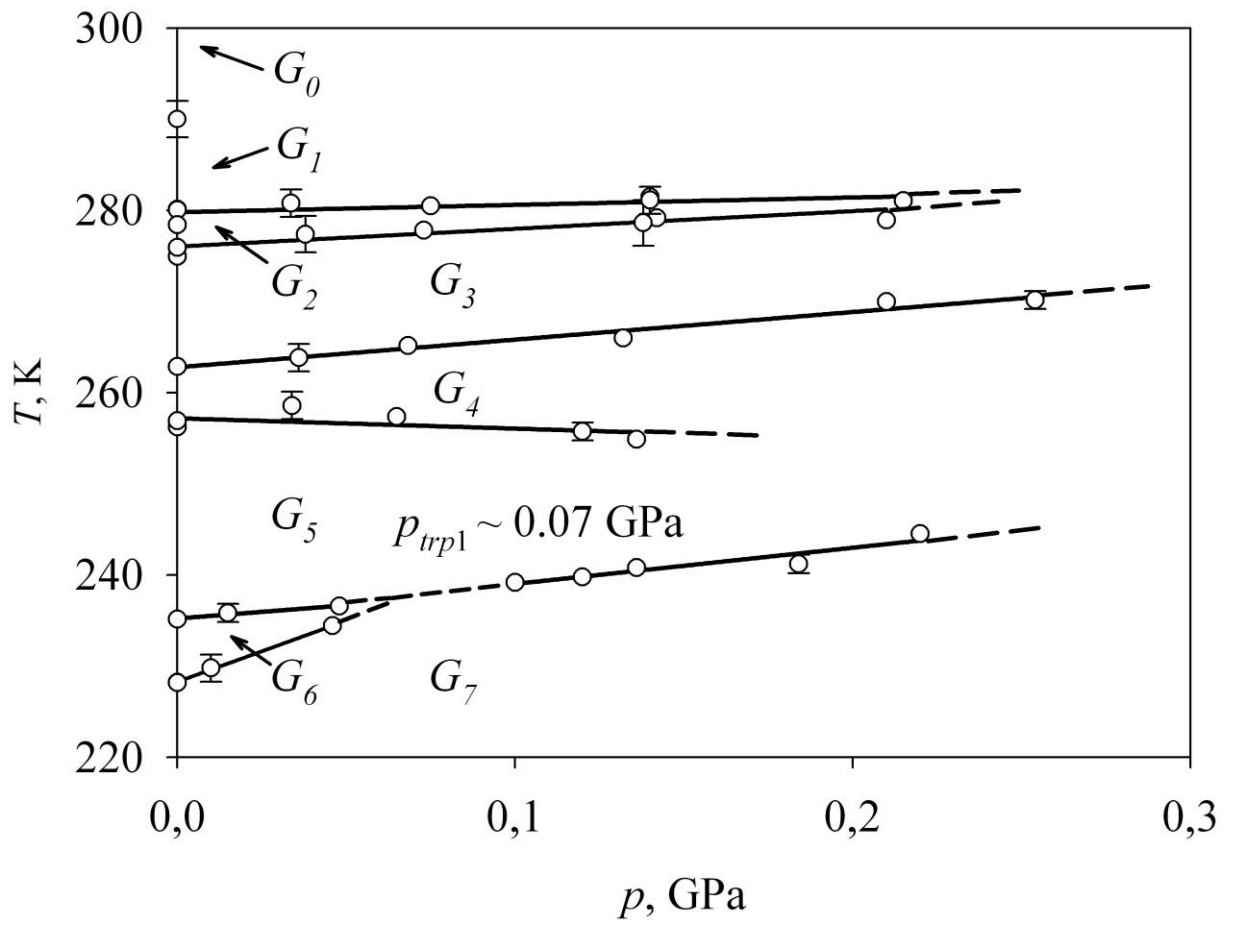


Fig. 2 Phase temperature-pressure diagram of the crystal (NH<sub>4</sub>)<sub>3</sub>HfF<sub>7</sub>.

Table 1 The baric coefficients of the phase transitions.

	$G_0 \leftrightarrow G_1$	$G_1 \leftrightarrow G_2$	$G_2 \leftrightarrow G_3$	$G_3 \leftrightarrow G_4$	$G_4 \leftrightarrow G_5$	$G_5 \leftrightarrow G_6$	$G_6 \leftrightarrow G_7$	$G_5 \leftrightarrow G_7$
$dT_i/dp,$ $K \cdot Gpa^{-1}$	-	8.0	19.5	30.4	-12.3	29.0	121.2	39.7

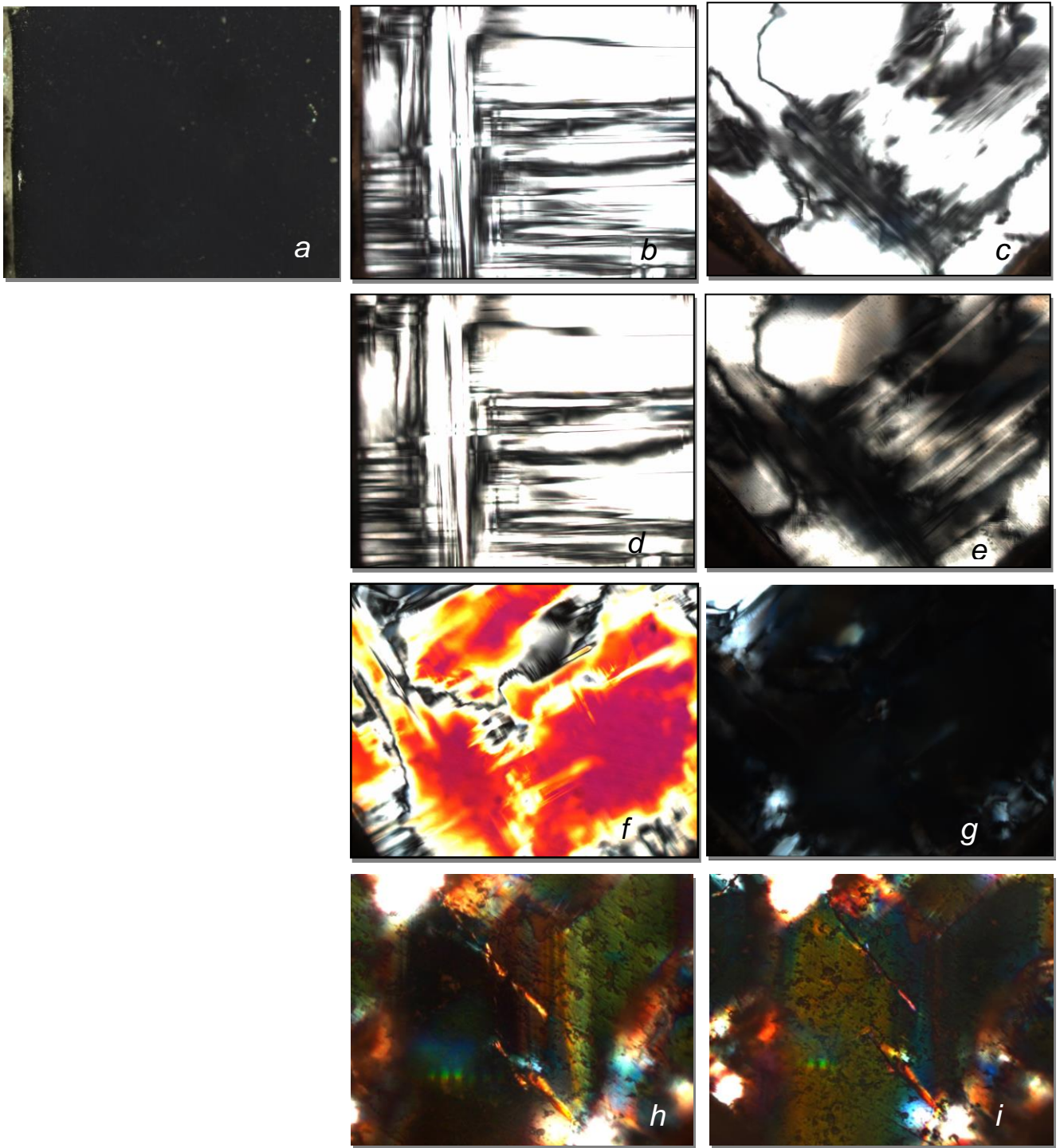


Fig. 3 Investigations in the polarized light on the cut  $(100)_c$  upon the cooling process. Phases (a) –  $(G_0, G_1)$ ; (b, c) –  $(G_2)$ ; (d, e) –  $(G_3)$ ; (f, g) –  $(G_4, G_5)$ ; (h, i) –  $(G_6, G_7)$

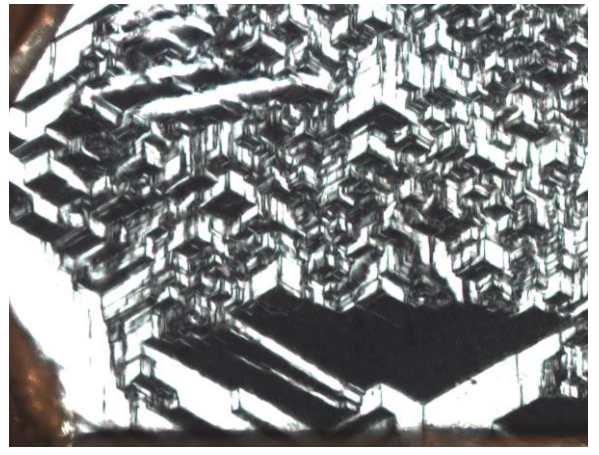
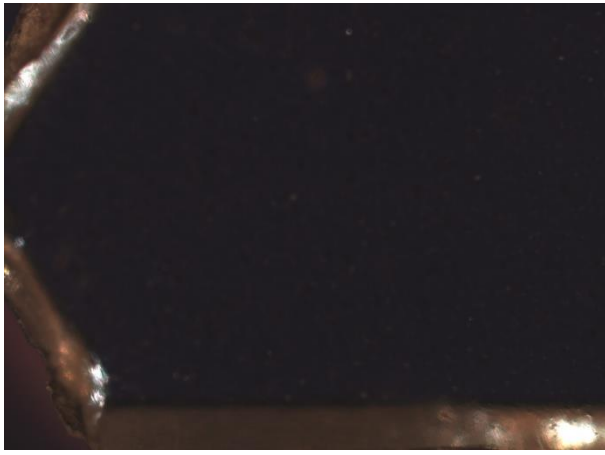


Fig. 4 Twinning in a cut  $(111)_c$ .

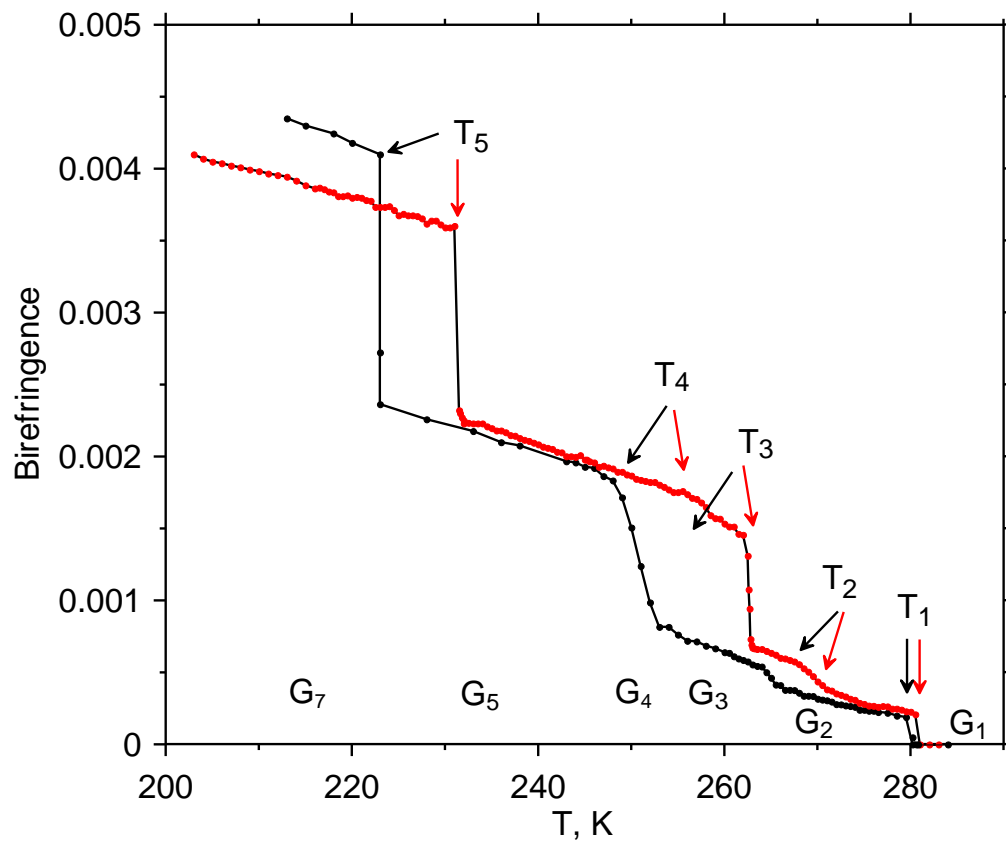


Fig. 5 Appearance, change and disappearance of birefringence in cut (001)<sub>c</sub> on heating (red dots) and cooling (black dots).

## Notes and references

- [1] I.N. Flerov, M.V. Gorev, K.S. Aleksandrov, A. Tressaud, J. Grannec, M. Couzi, Phase transitions in elpasolites (ordered perovskites), *Mater. Sci. Eng.* 24 (1998) 81-151.
- [2] W.Massa, G. Pausewang, Zur kristallstruktur von  $(\text{NH}_4)_3\text{Ti}(\text{O}_2)\text{F}_5$ , *Mat. Res. Bull.* 13 (1970) 361.
- [3] S.V. Mel'nikova, A. S. Krylov, A.L. Zhogal', N.M. Laptash, Optical studies of phase transitions in the  $(\text{NH}_4)_3\text{Ti}(\text{O}_2)\text{F}_5$  crystal, *Phys. Sol. State* 51 4 (2009) 817–822.
- [4] A.A. Udovenko, A.A. Karabtsov, N.M. Laptash, Crystallographic features of ammonium fluoro-elpasolites: dynamic orientational disorder in crystals of  $(\text{NH}_4)_3\text{HfF}_7$  and  $(\text{NH}_4)_3\text{Ti}(\text{O}_2)\text{F}_5$ , *Acta Cryst.* B73 (2017) 1–9 R.
- [5] R. Stomberg, I.B. Sveinsson, The Disordered Structure of Ammonium Pentafluoroperoxotitanate(IV),  $(\text{NH}_4)_3[\text{TiF}_5(\text{O}_2)]$ , *Acta Chem. Scand.* A31 (1977) 635.
- [6] D.L. Deadmore, W.F. Bradley, The crystal structure of  $\text{K}_3\text{SiF}_7$ , *Acta Cryst.* 15 (1962) 186-189.
- [7] J.L. Hoard, M.B. Williams, Structures of Complex Fluorides. Ammonium Hexafluorosilicate—Ammonium Fluoride,  $(\text{NH}_4)_2\text{SiF}_6 \cdot \text{NH}_4\text{F}$ , *J. Amer. Soc.* 64 (1942) 633-637.
- [8] C. Plitzko, G. Meyer, Crystal structure of triammonium heptafluorogermanate,  $(\text{NH}_4)_3\text{GeF}_7$ , *Z. Kristallogr. - New Cryst. Struct.* 213 (1998) 475.
- [9] C. Plitzko, G. Meyer, Kristallstruktur von  $(\text{NH}_4)_3\text{SnF}_7$ : Ein Doppelsalz gemäß  $(\text{NH}_4)_3[\text{SnF}_6]\text{F}$  und kein  $(\text{NH}_4)_4\text{SnF}_8$ , *Z. Anorg. Allg. Chem.* 623 (1997) 1347-1348.
- [10] U. Reusch, E. Schweda, In situ X-ray powder diffraction: The reaction of Pb(IV)-fluoride with ammonia and  $\text{NH}_4\text{F}$ , *Mater. Sci. For.* 378-381 (2001) 326-330.
- [11] S. V. Mel'nikova, M. S. Molokeev, N. M. Laptash, E. I. Pogoreltsev, S. V. Misyul, I. N. Flerov, Sequence of phase transitions in  $(\text{NH}_4)_3\text{SiF}_7$ , *Dalton Trans.* 46 (2017) 2609–2617.
- [12] H.J. Hurst, J.C. Taylor, A neutron diffraction analysis of the disorder in ammonium heptafluorozirconate, *Acta Cryst.* B26 (1970) 2136–2137
- [13] S.V. Misyul, S.V. Mel'nikova, A.F. Bovina, N.M. Laptash, Optical and x-ray diffraction studies of the symmetry of distorted phases of the  $(\text{NH}_4)_3\text{ZrF}_7$  crystal, *Phys. Solid State* **50** (2008) 1951–1956.
- [14] V.D. Fokina, M.V. Gorev, E.V. Bogdanov, E.I. Pogoreltsev, I.N. Flerov, N.M. Laptash, Thermal properties and phase transitions in  $(\text{NH}_4)_3\text{ZrF}_7$ , *J. Fluorine Chem.* 154 (2013) 1–6.